Proceedings of the ASME 2024
Turbomachinery Technical Conference & Exposition
GT2024
June 25–27, 2024, London, England, United Kingdom

GT2024-125954

UNDERSTANDING EBC LIFETIMES AND PERFORMANCE FOR INDUSTRIAL GAS TURBINES

M. J. Ridley[1], M. J. Lance[1], T. G. Aguirre[1], K. A. Kane[2], B. A. Pint[1]
[1]Materials Science and Technology Division, Oak Ridge National Laboratory, Oak Ridge, TN, USA
[2]Johns Hopkins University Applied Physics Laboratory, Laurel, MD, USA

ABSTRACT

Hydrogen or hydrogen blend fuels are expected to replace natural gas in land-based industrial gas turbines to support a greener power economy. With the increased hydrogen fuel costs, there is more incentive to increase turbine efficiency by increasing the turbine inlet temperature and decreasing the reliance on cooling air. The introduction of hydrogen is also expected to result in increased steam production as a combustion byproduct, necessitating introduction of structural components with increased thermochemical stability. Silicon carbide (SiC) base ceramic matrix composites (CMCs) are considered for replacement of Ni-based superalloys to accommodate such increases in hot gas temperature. SiC CMCs require environmental barrier coatings (EBCs) to mitigate volatilization from high-temperature steam, thus making the EBC lifetime critical information for identifying CMC component lifetimes. The goal of this project is to determine the maximum bond coating temperature underneath the EBC for achieving a component lifetime goal of 25,000 h, which is far greater than current CMC component lifetime requirements for aero-turbine applications. To provide data for the lifetime model, laboratory testing used plasma-sprayed rare-earth silicate EBCs on monolithic SiC substrates with an intermediate Si bond coating. Specimens exposed to 1-h thermal cycles in flowing air-steam environments and reaction kinetics were assessed from 1250°-1350°C by measuring the thickness of the thermally grown silica scales. The silica growth and phase transformation appear critical in predicting EBC lifetime and several strategies have been explored to reduce the oxide growth rate and improve EBC durability at elevated temperatures. Advanced characterization using Raman spectroscopy has helped clarify this system. This research was sponsored by the U. S. Department of Energy, Office of Fossil Energy and Carbon Management, Advanced Turbine Program.

Keywords: Environmental barrier coating; oxidation; durability

NOMENCLATURE

BSE	Backscattered Electron
CMC	Ceramic Matrix Composite
CVD	Chemical Vapor Deposition
EBC	Environmental Barrier Coating
IGT	Industrial Gas Turbine
SEM	Scanning Electron Microscopy
TBC	Thermal Barrier Coating
TGO	Thermally Grown Oxide

1. INTRODUCTION

SiC_{Fiber}/SiC_{Matrix} ceramic matrix composites (CMCs) have replaced select static aero turbine superalloy components to result in higher temperature capability, reduced component weight, and a resulting increase in turbine efficiency [1]. SiC/SiC CMCs improve turbine combustion temperatures and decrease reliance on cooling air through their high-temperature chemical stability and high strength from the SiC fiber weave. Yet, SiC is known to recede in the presence of steam due to the formation of $Si(OH)_4$ (g) from the SiO_2 thermally grown oxide (TGO) [2]. Environmental barrier coatings (EBCs) are required layers of protection against TGO volatilization. The lifetime of the EBC thus represents a critical measure of the operating lifetime for SiC components.

Industrial gas turbines (IGTs) for power generation do not currently utilize EBC/CMC components due to the decreased importance of low-density components compared to aero turbines. Large amounts of cooling air, engineered cooling channels, and thermal barrier coatings (TBCs) are instead employed to reduce the operating temperature of superalloy components [3]–[5]. Modern natural gas J-class turbines show promise to achieve 1700°C (3100°F) turbine inlet temperatures [6], necessitating the use of higher temperature materials within the combustor section. Additionally, the global shift towards low carbon or carbon-free fuels are expected to incentivize an introduction of EBC/CMC components into the IGT hot section. Interest in hydrogen and hydrogen blend fuels has resurged to

counteract global emissions, yet challenges such as high combustion temperatures, high steam content, flame stability, and energy density require both engineering design and high-temperature materials development for successful transition from natural gas [7]. Further, IGT component lifetimes are on the order of 25,000 h, where longer times at base load may impact EBC behavior relative to the more rapid temperature cycling associated with aero turbine flight patterns. A robust understanding of EBC durability and lifetime is needed for implementation of CMCs into the next generation of IGTs with low-carbon fuel sources.

2. MATERIALS AND METHODS

Chemical vapor deposition (CVD) SiC substrates (99.99% purity, Dow Chemical) were used as the sample substrates instead of SiC/SiC CMCs, as there is often a monolithic SiC outer layer on CMCs to protect the fiber weave. The CVD SiC substrates were grit blasted to produce local roughness for coating adhesion, followed by atmospheric plasma spray deposition of a standard silicon bond coating (36± 9 µm). Silicon and $Yb_2Si_2O_7$ powder feedstock were from Oerlikon Metco. The APS process resulted in some silica volatilization during particle flight through the plasma [8], resulting in a nominal chemistry of 60% $Yb_2Si_2O_7$ / 40% Yb_2SiO_5 and an EBC thickness of 173 ± 14 µm. After deposition, the specimens were annealed at 1300°C in laboratory air for 4 hours to crystallize and equilibrate the thermodynamically stable EBC phases.

Specimens were exposed for 1-h thermal cycles up to 1350°C in a horizontal tube furnace, with further details provided elsewhere [9]. The gas environment was 90% H_2O and 10% laboratory air flowing at 1.5 cm/s. Specimens were exposed at temperature in the gas environment for one hour, followed by rapid automated furnace removal of the specimens to room temperature laboratory air for 10 min. Specimens were exposed in 100, 300, and 500 cycles prior to removal for characterization. The resulting dataset was utilized to create an oxidation model, which was validated against specimen exposures at both 1250°C and 700°C thermal cycle temperatures.

Samples were characterized via resin mounting in cross-section and polishing to 0.25 µm with diamond suspension. Back-scattered electron (BSE) mode scanning electron microscopy (SEM) was performed on a TESCAN Mira3 to identify the EBC microstructure and TGO thickness after oxidation testing. An open source automated image analysis software was used to collect TGO thickness measurements over many millimeters of sample cross-section [10]. Sample edges were not included in the TGO thickness analysis to minimize specimen edge effects.

A heating stage was used in the SEM to look at the phase transformation of a thermally grown silica scale on a silicon wafer to visualize the magnitude of the phase change without the EBC. The Si wafer was oxidized for 100 h in air at 1350°C for visual evaluation of the SiO_2 phase transformation. High-temperature Raman (InVia, Renishaw, Inc.) with a 532 nm laser was used to analyze the chemical changes in cross-section on an EBC/SiO_2/Si/SiC specimen after exposure to 10 100-h cycles at 1350°C in the same gas environment as 1-h cycle testing discussed above. The specimen was mounted in resin, polished, sectioned, and finally removed from epoxy for characterization. A Linkam THMS600 stage was used to heat the polished specimen cross-section while collecting Raman spectra above and below the phase transformation temperature of the SiO_2 TGO. Principle component analysis was used to define phase fields from the spectra at each acquisition point to produce phase maps.

3. RESULTS AND DISCUSSION

3.1 Thermal Cycle Oxidation Testing

Cross-section SEM images of a specimen after the crystallization anneal in air are shown in Figure 1. Closed porosity was present in both the EBC and the Si bond coating from the thermal spray conditions utilized. Volatilization of the $Yb_2Si_2O_7$ powder feedstock during interaction with the plasma resulted in additional presence of Yb_2SiO_5 silica-depleted splats, highlighted in Figure 1b as the lighter greyscale splats.

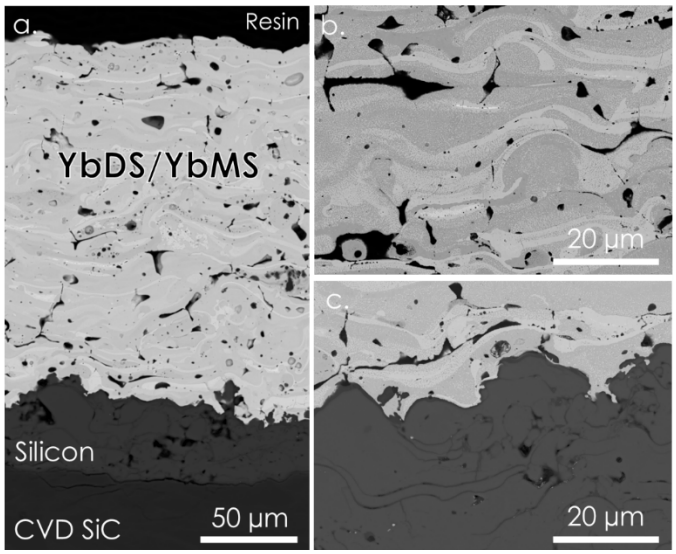

FIGURE 1. CROSS-SECTION BSE SEM IMAGES OF YBDS/YBMS EBC AFTER 4 H ANNEAL AT 1300°C IN STAGNANT LABORATORY AIR, A. FULL EBC/SI/SIC CROSS-SECTION, B. HIGHER MAGNIFICATION OF THE EBC, AND C. HIGHER MAGNIFICATION OF THE EBC-SI INTERFACE.

Figure 2 shows the EBC – Si interface after steam thermal cycling for 100, 300, or 500 1-h cycles at 1350°C. Minor coarsening of the Yb_2SiO_5 secondary phase in the EBC can be seen with time. SiO_2 growth under the EBC increases with time and the initial roughness and defects associated with the tortuous interface result in clear discontinuities in the TGO thickness. TGO thickness measurements for each exposure condition are also graphically displayed in Figure 2. A log-normal distribution was found, with increasing dynamic range of TGO thickness as exposure time increases. Resulting statistics can be found in Table 1. Both the mean and median TGO thicknesses (Figure 3) show parabolic growth kinetics with a reaction order near 2 (slope ~0.5), indicative of protective scale formation.

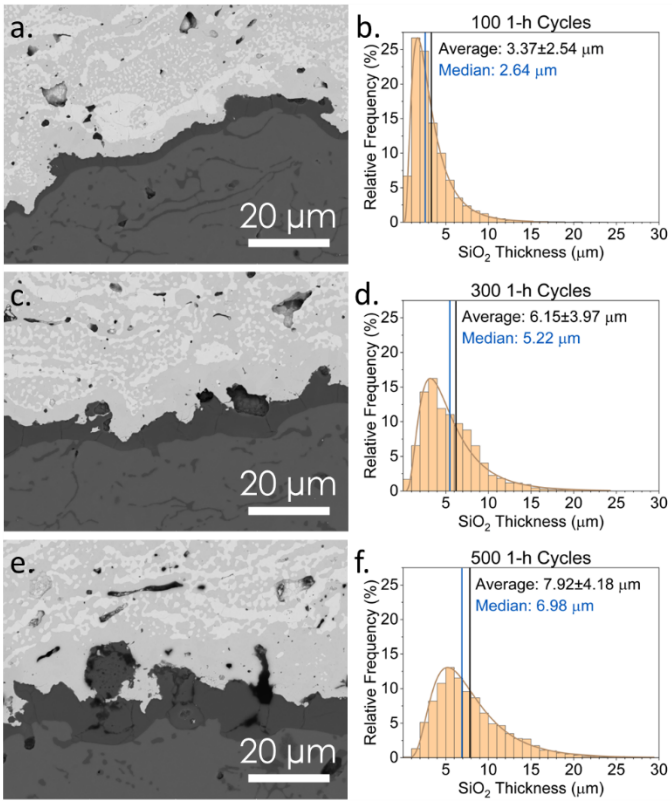

FIGURE 2. CROSS-SECTION BSE SEM IMAGES AND SCALE THICKNESS MEASUREMENTS OF THE SiO_2 TGO AFTER 1-H CYCLIC EXPOSURES AT 1350°C IN 90% H_2O (G) / 10% AIR FOR A,B. 100 CYCLES, C,D. 300 CYCLES, AND E,F. 500 CYCLES.

TABLE 1. STATISTICAL ANALYSIS OF SiO_2 TGO THICKNESS AFTER STEAM CYCLING.

	Cycle Time (h)		
	100	**300**	**500**
Mean (μm)	3.37 ± 2.54	6.15 ± 3.97	7.92 ± 4.18
Median (μm)	2.64	5.22	6.98
Counts	22,127	19,840	17,366
Distance (mm)	3.39	3.38	3.38

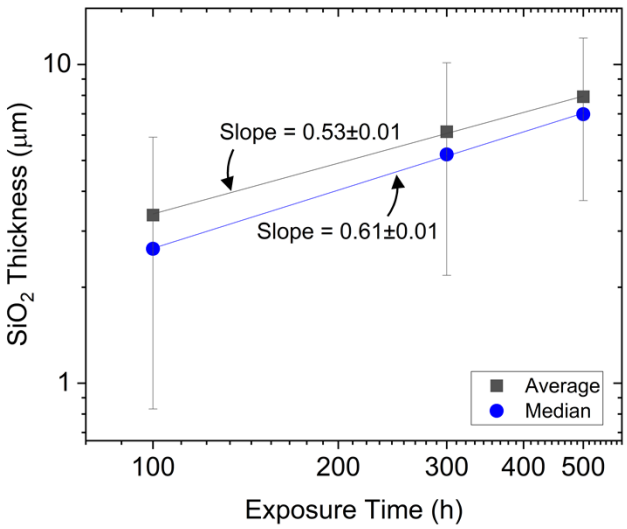

FIGURE 3. LOG-LOG PLOT OF SiO_2 SCALE THICKNESS.

3.2 Thermodynamic – Kinetic Oxidation Model

The resulting kinetic data at 1350°C were extrapolated both in time and temperature space to create a visualization of TGO layer thickness for extended use in IGTs. Deal and Grove provided wet air oxidation activation energy of Si to be 16.3 kcal/mol [11], approximated to 68 kJ/mol here. The color scale corresponds to predicted SiO_2 TGO thicknesses. Extrapolations were verified through comparison of other experimental data at 1250°C and 700°C, shown in Table 2. Given the relatively large standard deviation for scale thicknesses shown earlier in Table 1 and Figure 2, excellent agreement was found between the calculated and experimental SiO_2 thicknesses.

Slight deviation was found for the initial 700°C exposure, which may be related to the following effects. The kinetics may vary with inclusion of cycle times beyond 500 h, which would shift the expected oxidation kinetics for temperatures other than 1350°C. However, this effect is assumed negligible due to both the quality of the fit and by achieving a 2nd order reaction kinetics after 500 cycles of exposure. Previous work has shown that the temperature dependent rate for steam oxidation of Si under an EBC may be slightly higher than the value reported by Deal and Grove [11], which may result in a larger deviation with more extreme temperature differences such as extrapolation from 1350°C to 700°C. Furthermore, it is unclear if initial formation of a SiO_2 scale is amorphous or crystalline in the β-cristobalite phase, and such crystallinity differences may impact oxidant transport and subsequent growth rates. Finally, it is believed that the initial scale thickness may play a more dominant role when extrapolating down in temperature space, where very thin scales under 1 μm are present. Increased statistics may be required to appropriately assess TGO thicknesses for lower temperature exposures such as at 700°C.

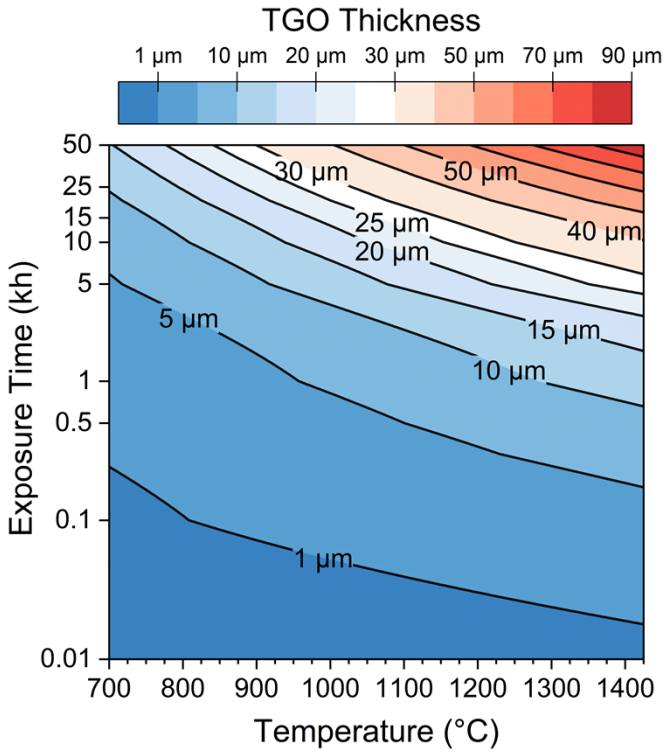

FIGURE 4. KINETIC MODEL FOR OXIDATION OF THE SI BOND COATING UNDER A YBDS/YBMS EBC BASED ON 1.5 CM/S FLOW OF 90% H_2O (G) / 10% AIR WITH 1-HOUR THERMAL CYCLING.

The current EBC/Si/SiC specimens had a Si bond coating with a thickness generally in the range of 30-40 µm. It can be assumed that a critical scale thickness for spallation is related to the total layer thickness. For example, full consumption of the Si bond coating to form SiO_2 is expected to result in rapid spallation. Yet, spallation may occur after a certain ratio of Si is consumed. If the average critical scale thickness is 20, 30 or 40 µm in thickness, then the maximum test temperature to achieve 25 kh is 880, 1030, or 1160°C, respectively. Typical EBC failure is often linked to EBC delamination at the EBC – SiO_2 interface [8], [12], indicating that SiO_2 formation drives coating failure. To appropriately define the failure criteria for EBC spallation, efforts have been directed towards understanding the behavior of SiO_2, as discussed below.

TABLE 2. MODEL VALIDATION TO OTHER TEST DATA. MEASURED DATA ARE AVERAGE SIO_2 THICKNESS. K_P IS THE OXIDATION RATE CONSTANT.

Temperature (°C)	Cycle Time (h)			k_p (µm²/h)
	100	300	500	
1350°C, Model	3.53	6.12	7.9	0.125
1350°C, Measured	3.4	6.15	7.9	0.125
1250°C, Model	3	5.19	6.7	0.09
1250°C, Measured	3.15	5.19	6.69	0.087
700°C, Model	0.66	1.14	1.47	0.0043
700°C, Measured	0.95	–	–	–

3.3 Failure Mode Identification

Additional characterization was performed on other sample sets to establish a baseline understanding of dominating failure mechanisms in the EBC/SiO_2/Si/SiC system, as such information can help refinement of an EBC lifetime model. High stresses have been associated with the SiO_2 phase change for cristobalite, which occurs usually between 230 and 270°C [13], [14]. To visualize this, a Si wafer was oxidized for 100 h in 90% H_2O (g) / 10% laboratory air at 1.5 cm/s to grow a SiO_2 TGO. The sample was placed on an angled (70°) heating stage in the SEM to witness material response through the phase change.

Figure 5 shows that the pre-existing mud cracks are present at room temperature due to a combination of SiO_2 growth, thermal, or phase transformation stresses. Upon heating in the SEM, cracks remain in focus despite the expected decrease in image quality associated with high-temperature SEM. Upon reaching 260°C, crack closure was evident, indicative of the α – β cristobalite phase transformation. The repeatable process of opening and closing existing cracks within SiO_2 suggests that the pre-existing mud cracks in SiO_2 likely remain closed at elevated exposure temperatures. For high temperatures and pressures within IGTs, it can be expected that creep and sintering may occur to further seal up fast pathways for oxidant transport. Further oxide growth, in addition to traversing through the phase change on cooling, are expected to re-open the crack network in addition to increasing the crack density.

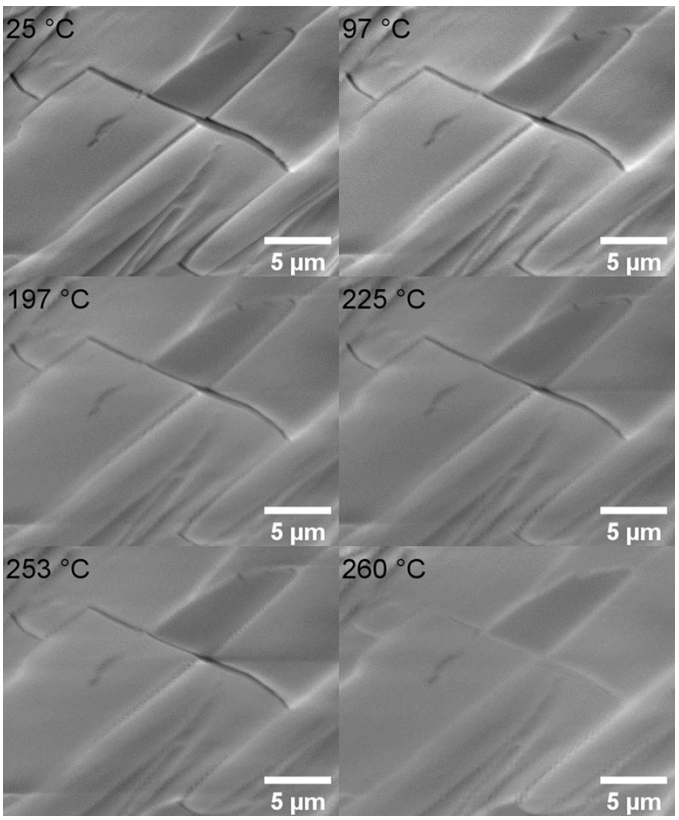

FIGURE 5. TEMPERATURE-DEPENDENT SEM IMAGES SHOWING CRACK CLOSURE IN THERMALLY GROWN SIO_2.

The SiO_2 phase transformation was also witnessed for the first time via high-temperature Raman on an exposed sample cross-section (10 100-h cycles, 1350°C, 90% H_2O), shown in Figure 6. An optical image of the sample cross-section is shown in Figure 6a. A thick and cracked SiO_2 scale is visible at the EBC – Si interface. Each subsequent phase was separated out with principal component analysis, resulting in the averaged spectra from each phase, Figure 6b. Raman spectra are in general agreement with the expected phases; the high intensity Si peak at 521 cm^{-1} was present with both cristobalite phases after principal component analysis due close proximity to the bond coat. Raman mapping was performed upon heating in air, where Figure 6c shows the cross-section at 260°C and Figure 6d shows the cross-section at 270°C, respectively. Clear distinction is found between the alpha and beta cristobalite phases, allowing for identification of the phase change. Without an EBC top layer, the SiO_2 phase change resulted in approximately 450 MPa stress buildup [14]. Peak shift calibrations are currently underway to quantify individual layer response based on both thermal and SiO_2 phase transformation stresses for specimen cross-sections after steam thermal cycling.

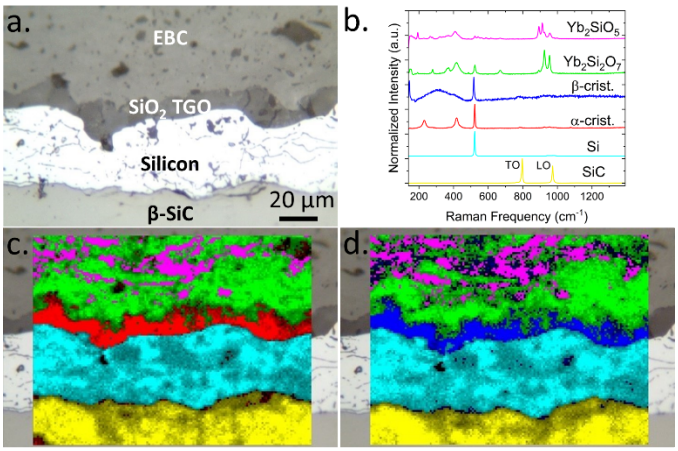

FIGURE 6. CROSS-SECTION OPTICAL IMAGES OF YBDS/YBMS EBC AFTER 1000H OF EXPOSURE AT 1350°C: A. ROOM TEMPERATURE, B. RAMAN SPECTRA FOR EACH PHASE, C. 260°C RAMAN PHASE MAP, AND D. 270°C RAMAN PHASE MAP.

3.4 Discussion

The oxidation kinetics of the Si bond coatings under $Yb_2Si_2O_7/Yb_2SiO_5$ EBCs shows parabolic growth rates with a temperature dependence in agreement with wet air Si oxidation. Thermal spray results in a rough and undulating EBC – Si interface, in addition to interfacial defects, which result in a lognormal SiO_2 thickness distribution after exposure up to 500 1-h cycles at 1350°C. After longer exposure times, the distribution may transition to a normal distribution. To better understand EBC durability, longer test durations are needed to acquire such data. Yet, laboratory testing of coupons with EBC deposition on a single side leaves edges exposed where direct oxidation of the Si at the EBC – Si interface can occur [12]. Accurate kinetic data can thus only be achieved up to a time where edge oxidation effects do not impact the oxidation at the center of the specimens. To achieve long-term kinetic data in support of a lifetime model, fully coated specimens should be considered for research purposes.

The lifetime model currently employs laboratory data at atmospheric pressure and a constant gas flow rate. Future efforts should include the expected total pressure, partial pressure, and gas velocity relationships within the model based on gas boundary layer theory and experimental validation.

Characterization has allowed for improved understanding of the SiO_2 layer properties as the primary failure mode for EBC oxidation in a thermally cycled environment. The α- to β-cristobalite phase transformation has been identified as a source for large stress buildup during thermal cycling which can induce cracking. The majority of cracks visible after testing are vertical segmentation cracks which are interconnected under the EBC to form a crack network. The crack density may play a critical role in the adhesion strength of the EBC, and the crack density relationship to SiO_2 thickness should be further investigated for definition of a critical scale thickness for EBC spallation. Contrarily, the witnessed crack closure upon heating without an EBC top coating may imply that cracks measured at room temperature may not result in fast transport of oxidant at elevated temperatures. The creep and sintering behavior of SiO_2 should also be investigated to improve understanding.

4. CONCLUSION

Thermal cycle testing of EBC/Si/SiC coupons was performed at 1350°C to develop an updated visual model for the time and temperature evolution of SiO_2 formation. The model was validated against experimental testing at 1250°C and 700°C. Insights on the SiO_2 TGO durability were revealed through further characterization, where the SiO_2 phase transformation was identified as a dominant failure point for EBCs.

ACKNOWLEDGEMENTS

The authors acknowledge J. Wade, Y.F. Su and J. Horenburg for experimentation and characterization support at ORNL, T. Koyanagi for support with the SEM heating stage, B. Lamm and S. Bell for technical review. Access to the Raman spectrometer was provided by the Nuclear Nonproliferation Division at ORNL. This research was sponsored by the U. S. Department of Energy, Office of Fossil Energy and Carbon Management, Advanced Turbine Program.

This manuscript has been authored by UT-Battelle, LLC under Contract No. DE-AC05-00OR22725 with the U.S. Department of Energy. The United States Government retains and the publisher, by accepting the article for publication, acknowledges that the United States Government retains a non-exclusive, paid-up, irrevocable, world-wide license to publish or reproduce the published form of this manuscript, or allow others to do so, for United States Government purposes. The Department of Energy will provide public access to these results of federally sponsored research in accordance with the DOE Public Access Plan (http://energy.gov/downloads/doe-public-access-plan).

REFERENCES

[1] G. Gardiner, “Aeroengine Composites, Part 1: The CMC invasion,” *Compos. World*, 2015, [Online]. Available: compositesworld.com/articles/aeroengine-composites-part-1-the-cmc-invasion

[2] E. J. Opila, “Oxidation and Volatilization of Silica Formers in Water Vapor,” *J. Am. Ceram. Soc.*, vol. 86, no. 8, pp. 1238–1248, Aug. 2003, doi: 10.1111/j.1151-2916.2003.tb03459.x.

[3] B. Gleeson, “Thermal Barrier Coatings for Aeroengine Applications,” *J. Propuls. Power*, vol. 22, no. 2, pp. 375–383, Mar. 2006, doi: 10.2514/1.20734.

[4] V. Kumar and K. Balasubramanian, “Progress update on failure mechanisms of advanced thermal barrier coatings: A review,” *Prog. Org. Coat.*, vol. 90, pp. 54–82, Jan. 2016, doi: 10.1016/j.porgcoat.2015.09.019.

[5] F. N. Nourin and R. S. Amano, “Review of Gas Turbine Internal Cooling Improvement Technology,” *J. Energy Resour. Technol.*, vol. 143, no. 080801, Nov. 2020, doi: 10.1115/1.4048865.

[6] K. Suzuki, Y. Matsumura, K. Takata, S. Hada, M. Yuri, and J. Masada, “Evolution of MHPS Large Frame Gas Turbines: J to Air-Cooled JAC,” presented at the ASME Turbo Expo 2018: Turbomachinery Technical Conference and Exposition, American Society of Mechanical Engineers Digital Collection, Aug. 2018. doi: 10.1115/GT2018-77273.

[7] E. Stefan, B. Talic, Y. Larring, A. Gruber, and T. A. Peters, “Materials challenges in hydrogen-fuelled gas turbines,” *Int. Mater. Rev.*, vol. 67, no. 5, pp. 461–486, Jul. 2022, doi: 10.1080/09506608.2021.1981706.

[8] M. Ridley, E. Garcia, K. Kane, S. Sampath, and B. Pint, “Environmental barrier coatings on enhanced roughness SiC: Effect of plasma spraying conditions on properties and performance,” *J. Eur. Ceram. Soc.*, vol. 43, no. 14, pp. 6473–6481, Nov. 2023, doi: 10.1016/j.jeurceramsoc.2023.06.049.

[9] M. Ridley *et al.*, “Steam oxidation and microstructural evolution of rare earth silicate environmental barrier coatings,” *J. Am. Ceram. Soc.*, vol. 106, no. 1, pp. 613–620, Jan. 2023, doi: 10.1111/jace.18769.

[10] Y. F. Su *et al.*, “Quantifying High Temperature Corrosion,” presented at the NACE CORROSION, NACE CORROSION. OnePetro, Apr. 2021. Accessed: Jul. 27, 2022. [Online]. Available: https://onepetro.org/NACECORR/proceedings/CORR21/2-CORR21/D021S009R005/464033

[11] B. E. Deal and A. S. Grove, “General Relationship for the Thermal Oxidation of Silicon,” *J. Appl. Phys.*, vol. 36, no. 12, pp. 3770–3778, Dec. 1965, doi: 10.1063/1.1713945.

[12] K. Kane, E. Garcia, M. Lance, C. Parker, S. Sampath, and B. Pint, “Accelerated oxidation during 1350°C cycling of ytterbium silicate environmental barrier coatings,” *J. Am. Ceram. Soc.*, vol. 105, no. 4, pp. 2754–2763, Dec. 2021, doi: 10.1111/jace.18231.

[13] A. J. Leadbetter and A. F. Wright, “The α—β transition in the cristobalite phases of SiO_2 and $AlPO_4$ I. X-ray studies,” *Philos. Mag. J. Theor. Exp. Appl. Phys.*, vol. 33, no. 1, pp. 105–112, Jan. 1976, doi: 10.1080/14786437608221095.

[14] M. J. Lance, M. J. Ridley, K. A. Kane, and B. A. Pint, “Raman spectroscopic characterization of SiO_2 phase transformation and Si substrate stress relevant to EBC performance,” *J. Am. Ceram. Soc.*, vol. 106, no. 10, pp. 6205–6210, 2023, doi: 10.1111/jace.19190.

